THE JOURNAL OF BIOLOGICAL CHEMISTRY
Vol. 278, No. 19, Issue of May 9, pp. 17546–17556, 2003

Printed in U.S.A.

Activation of Muscarinic Receptors Inhibits β-Amyloid Peptide-induced Signaling in Cortical Slices*

Received for publication, September 26, 2002, and in revised form, January 31, 2003
Published, JBC Papers in Press, February 26, 2003, DOI 10.1074/jbc.M209892200

Zhenglin Gu, Ping Zhong, and Zhen Yan‡

From the Department of Physiology and Biophysics, State University of New York at Buffalo, School of Medicine and Biomedical Sciences, Buffalo, New York 14214

Deposition of fibrillar aggregates of the β-amyloid peptide (Aβ) is a key pathologic feature during the early stage of Alzheimer's disease. The initial neuronal responses to Aβ in cortical circuits and the regulation of Aβ-induced signaling remain unclear. In this study, we found that exposure of cortical slices to $A\beta_{1-42}$ or $A\beta_{25-35}$ induced a marked increase in the activation of protein kinase C (PKC) and Ca^{2+}/calmodulin-dependent kinase II (CaMKII), two enzymes critically involved in a variety of cellular functions. Activation of M1 muscarinic receptors, but not nicotinic receptors, significantly inhibited the Aβ activation of PKC and CaMKII. Increasing inhibitory transmission mimicked the M1 effect on Aβ, whereas blocking $GABA_A$ receptors eliminated the M1 action. Moreover, electrophysiological evidence shows that application of Aβ to cortical slices induced action potential firing and enhanced excitatory postsynaptic currents, whereas muscarinic agonists potently increased inhibitory postsynaptic currents. These results suggest that Aβ activates PKC and CaMKII through enhancing excitatory activity in glutamatergic synaptic networks. Activation of M1 receptors inhibits Aβ signaling by enhancing the counteracting $GABA_{ergic}$ inhibitory transmission. Thus the muscarinic reversal of the Aβ-induced biochemical and physiological changes provides a potential mechanism for the treatment of Alzheimer's disease with cholinergic enhancers.

The 40–42-amino acid β-amyloid peptide (Aβ)[1] is a major constituent of senile plaques (1), extracellular protein aggregates that are used as a histopathological hallmark for the diagnosis of Alzheimer's disease (AD). Emerging evidence has suggested that Aβ makes a direct contribution to the pathogenesis of AD (2, 3). Aβ peptides are produced by the cleavage of β-amyloid precursor protein (APP) (4). Mutations in the APP gene increases the rate of cleavage, thereby leading to the overproduction of Aβ (5, 6). Transgenic mice overexpressing mutant APP genes exhibit AD-like Aβ deposits and cognition impairments (7–9). *In vitro* studies in cell lines and cultured neurons show that fibrillar Aβ is neurotoxic at high concentrations (10, 11), and most strikingly, Aβ exposure renders neurons more vulnerable to excitatoxicity (12, 13). Although intensive efforts have been concentrated on factors affecting Aβ production, aggregation, and metabolism (14, 15), little is known about the earliest biochemical and physiological changes in neurons in response to the subtoxic concentrations of Aβ, which may be critical for subsequent neurodegenerative changes and the factors that can regulate the Aβ-initiated signaling.

In addition to Aβ deposits, a prominent feature of AD is the degeneration of basal forebrain cholinergic neurons and ensuing deficient cholinergic functions in their target areas including cortex and hippocampus (16–18). Despite an improved understanding of the critical role of the cholinergic system in normal cognition and dementia (19, 20), it has been largely unclear how cholinergic deficits and Aβ accumulation might be related to each other. Previous evidence suggests that Aβ can induce cholinergic hypofunction independently of apparent neurotoxicity (21), whereas activation of muscarinic receptors can inhibit the generation of amyloidogenic Aβ (22, 23), indicative of a reciprocal negative regulation between them.

Here we report that treatment of cortical slices with Aβ led to a rapid increase in the activation of protein kinase C (PKC) and Ca^{2+}/calmodulin-dependent kinase II (CaMKII), and this effect was dependent on Aβ-induced excitation of glutamatergic synapses and ensuing Ca^{2+} influx. Furthermore, the Aβ signaling was selectively down-regulated by the activation of muscarinic receptors through a mechanism involving enhanced GABAergic inhibition. Given the key roles of PKC and CaMKII in regulating a wide range of neuronal functions from synaptic plasticity to cell survival (24, 25), their strong activation by Aβ could interfere with these critical processes and thereby might contribute to cognitive deficits in AD. The ability of muscarinic receptors to block the Aβ signaling provides one potential mechanism supporting the notion that enhancing cholinergic transmission could be an effective therapeutic strategy in AD treatment (26, 27).

MATERIALS AND METHODS

Western Blot Analysis—Young adult (3–5 weeks postnatal) rat slices containing frontal cortex were prepared as previously described (28, 29). All of the experiments were carried out according to the Yroval of State University of New York at Buffalo Animal Care Committee. In brief, the rats were anesthetized by inhaling 2-bromo-2-chloro-1,1,1-trifluoroethane (1 ml/100 g; Sigma) and decapitated; the brains were quickly removed, iced, and then blocked for slicing. The blocked tissue

* This work was supported by National Science Foundation Grant IBN-0117026 (to Z. Y.), National Institutes of Health Grant MH63128 (to Z. Y.), and Howard Hughes Medical Institute Biomedical Research Support Program Grant 53000261 (to SUNY at Buffalo). The costs of publication of this article were defrayed in part by the payment of page charges. This article must therefore be hereby marked "*advertisement*" in accordance with 18 U.S.C. Section 1734 solely to indicate this fact.

‡ To whom correspondence should be addressed: Dept. of Physiology and Biophysics, State University of New York at Buffalo, 124 Sherman Hall, Buffalo, NY 14214. E-mail: zhenyan@buffalo.edu.

[1] The abbreviations used are: Aβ, β-amyloid peptide; AD, Alzheimer's disease; APP, β-amyloid precursor protein; PKC, protein kinase C; CaMKII, Ca^{2+}/calmodulin-dependent kinase II; GABA, γ-aminobutyric acid; ANOVA, analysis of variance; oxo-M, oxotremorine methiodide; MK-801, (+)-5-methyl-10,11-dihydro-5H-dibenzo[a,d] cyclohepten-5,10-imine maleate; CNQX, 6-cyano-7-nitroquinoxaline-2,3-dione; MT-7, muscarinic toxin 7; sEPSC, spontaneous excitatory postsynaptic current; sIPSC, spontaneous inhibitory postsynaptic current; NMDA, *N*-methyl-D-aspartate; TTX, tetrodotoxin; AMPA, α-amino-3-hydroxy-5-methyl-4-isoxazolepropionic acid; KA, kainic acid/kainate; K-S, Kolmogorov-Smirnov; VDCC, voltage-dependent Ca^{2+} channel; mAChR, muscarinic cholinergic receptor; nAChR, nicotinic cholinergic receptor.

was cut in 300–400-μm slices with a Vibrotome while being bathed in a low Ca^{2+} (100 μM), HEPES-buffered salt solution (140 mM sodium isethionate, 2 mM KCl, 4 mM $MgCl_2$, 0.1 mM $CaCl_2$, 23 mM glucose, 15 mM HEPES, 1 mM kynurenic acid, pH 7.4, osmolarity = 300–305). The slices were then incubated for 1 h at room temperature (20–22 °C) in a $NaHCO_3$-buffered saline bubbled with 95% O_2, 5% CO_2 (126 mM NaCl, 2.5 mM KCl, 2 mM $CaCl_2$, 2 mM $MgCl_2$, 26 mM $NaHCO_3$, 1.25 mM NaH_2PO_4, 10 mM glucose, 1 mM pyruvic acid, 0.05 mM glutathione, 0.1 mM N^G-nitro-L-arginine, 1 mM kynurenic acid, pH 7.4; osmolarity = 300–305). All of the reagents were obtained from Sigma.

For detecting activated PKC, a phospho-PKC (pan) antibody that recognizes PKCα, β_I, β_{II}, ε, η, and δ isoforms only when phosphorylated at a carboxyl-terminal residue homologous to Ser^{660} of PKCβ_{II} was used in the Western blot analysis. Activated CaMKII was detected with an antibody recognizing the Thr^{286}-phosphorylated CaMKII. After incubation, the slices were transferred to boiling 1% SDS and homogenized immediately. Insoluble material was removed by centrifugation (13,000 × *g* for 10 min), and the protein concentration for each sample was measured. To minimize slice variations, pairs of coronal sections were compared. Equal amounts of protein from slice homogenates were separated on 7.5% acrylamide gels and transferred to nitrocellulose membranes. The blots were blocked with 5% nonfat dry milk for 1 h at room temperature. Then the blots were incubated with the phospho-PKC (pan) antibody (Cell Signaling, 1:2000) or the anti-Thr^{286}-phosphorylated CaMKII antibody (Promega, 1:2,000) for 1 h at room temperature. After being rinsed, the blots were incubated with horseradish peroxidase-conjugated anti-rabbit antibodies (Amersham Biosciences; 1:2000) for 1 h at room temperature. Following three washes, the blots were exposed to the enhanced chemiluminescence substrate. Then the blots were stripped for 1 h at 50 °C followed by saturation in 5% nonfat dry milk and incubated with a PKC antibody (Santa Cruz, 1:2000) recognizing the α, β, and γ isoforms or an anti-CaMKII antibody (Upstate Biotechnology Inc.; 1:2000). Quantitation was obtained from densitometric measurements of immunoreactive bands on autoradiograms. The data correspond to the means ± S.D. of 5–10 samples/condition and were analyzed by ANOVA tests.

Cholinergic receptor ligands oxotremorine methiodide (oxo-M), pirenzepine, methoctramine, nicotine, as well as channel blockers or activators (+)-5-methyl-10,11-dihydro-5H-dibenzo[a,d] cycloheptene-5,10-imine maleate (MK-801), 6-cyano-7-nitroquinoxaline-2,3-dione (CNQX), D(−)-2-amino-5-phosphonopetanoic acid (D-APV), nifedipine, diazepam (Sigma) were made up as concentrated stocks in water and stored at −20 °C. The selective ligand for M1 receptors, muscarinic toxin 7 (MT-7), was obtained from Peptides International (Louisville, KY). The stocks were thawed and diluted immediately prior to use. The β-amyloid peptide $A\beta_{25-35}$, the control peptide containing the reverse sequence $A\beta_{35-25}$, the full-length peptide $A\beta_{1-42}$, $A\beta_{1-40}$, and the control peptide containing the reverse sequence $A\beta_{40-1}$ were obtained from Sigma. $A\beta_{25-35}$ and $A\beta_{35-25}$ were resuspended in sterile distilled water at a concentration of 2 mM and incubated at 37 °C for 1 h to allow fibril formation (30). $A\beta_{1-42}$, $A\beta_{1-40}$, and $A\beta_{40-1}$ were resuspended in 50% phosphate-buffered saline at a concentration of 1.5 mg/ml and incubated at 37 °C for 4–7 days to allow fibril formation (31).

Protein Kinase Assay—After incubation, the brain slices were lysed in cold lysis buffer (1% Triton X-100, 5 mM EDTA, 10 mM Tris, 50 mM NaCl, 30 mM $Na_4P_2O_7 \cdot 10H_2O$, 50 mM NaF, 0.1 mM Na_3VO_4, 1 mM phenylmethylsulfonyl fluoride, Complete protease inhibitors from Roche Applied Science) on ice for 30 min. The brain lysates were centrifuged and ultracentrifuged, and PKC was immunoprecipitated with mouse monoclonal anti-PKCαβγ (Santa Cruz Biotechnology, Santa Cruz, CA) for 1 h, followed by the addition of 50 μl of protein A-Sepharose beads and incubation for 1 h at 4 °C. The beads were pelleted by centrifugation and washed three times with lysis buffer and three times with kinase buffer (50 mM Tris-HCl, pH 7.5, 5 mM $MgCl_2$) and then resuspended in 30 μl of kinase buffer. *In vitro* kinase activity was measured in the PKC immunoprecipitates using myelin basic protein as substrate. The assay was initiated by the addition of 1 μl of [γ-^{32}P]ATP (10 mCi/ml), 4 μl of ATP (100 μM), and 1 μl of myelin basic protein (5 mg/ml), continued for 20 min at room temperature, and stopped by boiling samples in SDS/PAGE sample buffer. The samples were loaded onto a 20% polyacrylamide gel and subjected to electrophoresis. The gels were vacuum-dried and exposed to Biomax film. The kinase activity was quantified by PhosphorImager.

Electrophysiological Recordings in Slices—To evaluate the regulation of neuronal excitability by $A\beta_{25-35}$ in frontal cortical slices, the whole cell current clamp recordings were used with patch electrodes (5–9 MΩ) filled with the following internal solution 60 mM K_2SO_4, 60 mM *N*-methyl-D-glucamine, 40 mM HEPES, 4 mM $MgCl_2$, 5 mM 1,2-bis(2-aminophenoxy)ethane-*N*,*N*,*N*′,*N*′-tetraacetic acid (BAPTA), 12 mM phosphocreatine, 2 mM Na_2ATP, 0.2 mM Na_3GTP, 0.1 mM leupeptin, pH 7.2–7.3 (osmolarity = 265–270). For the measurement of spontaneous excitatory postsynaptic currents (sEPSCs) in slices, the whole cell voltage clamp recordings were used with the following internal solution: 130 mM cesium methanesulfonate, 10 mM CsCl, 4 mM NaCl, 10 mM HEPES, 1 mM $MgCl_2$, 5 mM EGTA, 12 mM phosphocreatine, 5 mM MgATP, 0.2 mM Na_3GTP, 0.1 mM leupeptin, pH 7.2–7.3 (osmolarity = 265–270). The $GABA_A$ receptor antagonist bicuculline (10 μM) was added to the recording solution to block the inhibitory transmission. For the measurement of spontaneous inhibitory postsynaptic currents (sIPSCs), the whole cell voltage clamp internal solution contained 100 mM CsCl, 30 mM *N*-methyl-D-glucamine, 10 mM HEPES, 1 mM $MgCl_2$, 4 mM NaCl, 5 mM EGTA, 12 mM phosphocreatine, 2 mM MgATP, 0.2 mM Na_3GTP, 0.1 mM leupeptin, pH 7.2–7.3 (265–270 mosmol/liter). The AMPA/KA receptor antagonist CNQX (10 μM) and NMDA receptor antagonist D(−)-2-amino-5-phosphonopetanoic acid (25 μM) were added to the recording solution to block glutamate transmission. The slice (300 μm) was placed in a perfusion chamber attached to the fixed stage of an upright microscope (Olympus) and submerged in continuously flowing oxygenated artificial cerebrospinal fluid. The cells were visualized with a 40× water immersion lens and illuminated with near infrared light, and the image was detected with an infrared-sensitive CCD camera. A Multiclamp 700A amplifier (Axon Instruments, Union City, CA) was used for these recordings. Tight seals (2–10 GΩ) from visualized pyramidal neurons were obtained by applying negative pressure. The membrane was disrupted with additional suction, and the whole cell configuration was obtained. The access resistances ranged from 13 to 18 MΩ and were compensated 50–70%. The cells were held at −70 mV for the recording of spontaneous EPSCs or IPSCs. The Mini Analysis Program (Synaptosoft, Leonia, NJ) was used to analyze synaptic activity. Synaptic currents of 1 min (200–1000 events) under each different treatment were used for analysis. Statistical comparisons of the synaptic currents were made using the Kolmogorov-Smirnov (K-S) test.

RESULTS

Exposure of Cortical Slices to Aβ Increased PKC and CaMKII Activation in a Time- and Dose-dependent Manner—To identify possible early cellular responses to Aβ treatment that precede cell death, we examined the effect of Aβ peptides on the activation of two important serine/threonine kinases, PKC and CaMKII, in cortical slices. Because the catalytic competence of many PKC isozymes depends on autophosphorylation at the carboxyl terminus on a conserved residue (32), a phosphospecific pan PKC antibody that detects PKC isoforms only when phosphorylated at this residue was used to detect activated PKC. CaMKII is autophosphorylated at Thr^{286} when the enzyme is activated in the presence of Ca^{2+}/calmodulin, leading to the appearance of a sustained Ca^{2+}-independent activity (33, 34); thus an anti-Thr^{286}-phosphorylated CaMKII antibody was used to detect activated CaMKII.

$A\beta_{25-35}$, which represents the biologically active region of Aβ (35–37), was aged to produce aggregated $A\beta_{25-35}$. Application of aged $A\beta_{25-35}$ (10 μM) to cortical slices induced a marked increase in the activated PKC and CaMKII. The dose dependence of $A\beta_{25-35}$-induced PKC and CaMKII activation is shown in Fig. 1 (*A* and *B*). A small effect could be detected following a 10-min exposure to low concentrations of aged $A\beta_{25-35}$ (0.1–1 μM), and a saturating effect was seen at 10 μM of $A\beta_{25-35}$. The total PKC and CaMKII levels exhibited no change with the $A\beta_{25-35}$ treatment (Fig. 1*A*). Quantification data exhibited a 5.2 ± 1.2-fold increase of PKC ($n = 12$, $p < 0.001$, ANOVA) and a 6.2 ± 1.2-fold increase of CaMKII ($n = 12$, $p < 0.001$, ANOVA) following a 10-min exposure to aged $A\beta_{25-35}$ (10 μM; Fig. 1*B*). Similarly, the full-length fibrillar Aβ peptide, $A\beta_{1-42}$, also induced a potent increase in the activated PKC and CaMKII. The dose dependence of $A\beta_{1-42}$-induced PKC and CaMKII activation is shown in Fig. 1*C*. A small effect was detectable following a 10-min exposure to 0.1 μM of aged $A\beta_{1-42}$, and a saturating effect was observed at 1 μM of $A\beta_{1-42}$. Quantification data exhibited a 5.0 ± 1.0-fold increase of PKC

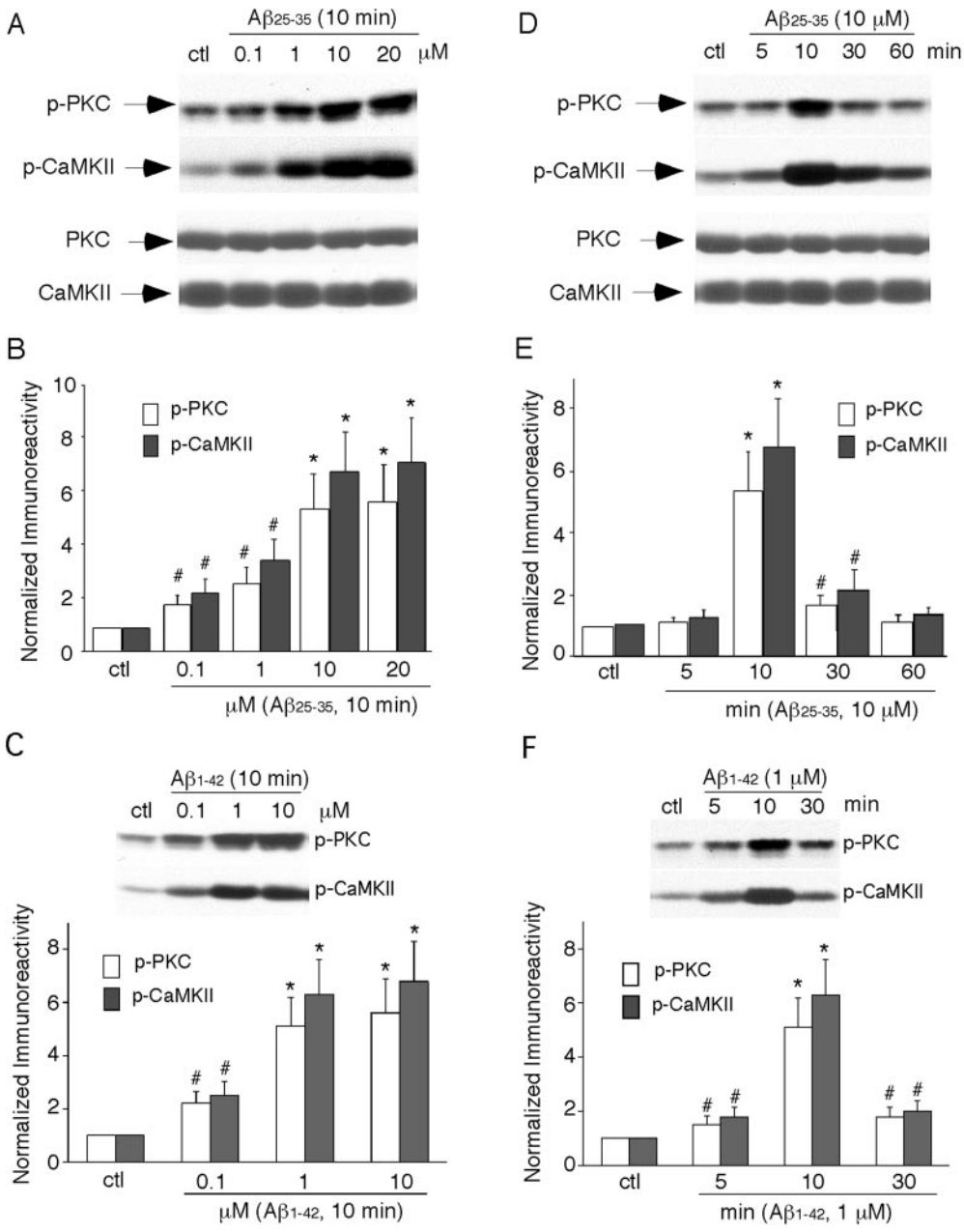

FIG. 1. **Activation of PKC and CaMKII by fibril Aβ: potency and kinetics.** *A*, dose dependence of the $A\beta_{25-35}$-induced phosphorylation of PKC and CaMKII. The slices were treated with $A\beta_{25-35}$ for 10 min at the indicated concentrations. Extracts of the slices were immunoblotted with an anti-phospho-PKC or an anti-phospho-CaMKII antibody, followed by reblotting with antibodies recognizing the total PKC or CaMKII. *B*, quantitation of PKC and CaMKII phosphorylation induced by different concentrations of $A\beta_{25-35}$. *C*, quantitation from four experiments showing the dose dependence of the $A\beta_{1-42}$-induced phosphorylation of PKC and CaMKII. *Inset*, representative immunoblots from one experiment. *D*, time course of the $A\beta_{25-35}$-induced phosphorylation of PKC and CaMKII. The brain slices were incubated in the absence or presence of aged $A\beta_{25-35}$ (10 μM) for the indicated times, and phospho-PKC and phospho-CaMKII were detected by immunoblotting of slice extracts. *E*, quantitation of PKC and CaMKII phosphorylation induced by $A\beta_{25-35}$ treatment for different lengths of time. *F*, quantitation from three experiments showing the time course of the $A\beta_{1-42}$-induced phosphorylation of PKC and CaMKII. *Inset*, representative immunoblots from one experiment. *, $p < 0.001$; #, $p < 0.01$, ANOVA, compared with control. *ctl*, control.

($n = 4$, $p < 0.001$, ANOVA) and a 6.1 ± 1.1-fold increase of CaMKII ($n = 4$, $p < 0.001$, ANOVA) following a 10-min exposure to aged $A\beta_{1-42}$ (1 μM; Fig. 1*C*). A representative example is shown in Fig. 1*C* (*inset*). These results suggest that $A\beta_{1-42}$ is more potent than $A\beta_{25-35}$ in activating PKC and CaMKII.

The kinetics of Aβ-induced activation of PKC and CaMKII was also tested. As demonstrated in Fig. 1 (*D–F*), The PKC and CaMKII activation induced by $A\beta_{25-35}$ (10 μM) or $A\beta_{1-42}$ (1 μM) showed rapid and transient kinetics, reaching a peak at 10 min and declining to basal levels within 30–60 min. In contrast to the potent activation of PKC and CaMKII by $A\beta_{25-35}$ in cortical slices, $A\beta_{25-35}$ failed to elicit the effect in striatal slices ($n = 5$; data not shown). Given such a time and dose dependence of the Aβ effect on PKC and CaMKII activation, the following experiments were performed with a 10-min treatment of $A\beta_{25-35}$ (10 μM) or $A\beta_{1-42}$ (1 μM) in frontal cortical slices unless otherwise stated.

We then compared the effect of different Aβ peptides on PKC and CaMKII activation. As shown in Fig. 2 (*A* and *B*), the 10-min treatment with unaged $A\beta_{25-35}$ peptide (10 μM) also induced a significant increase in activated PKC (2.9 ± 0.55-fold, $n = 6$, $p < 0.01$, ANOVA) and CaMKII (3.8 ± 0.78-fold, $n = 6$, $p < 0.01$, ANOVA), but to a lesser extent than aged $A\beta_{25-35}$ (10 μM) (PKC, 5.4 ± 1.3-fold; CaMKII, 6.8 ± 1.5-fold; $n = 10$,

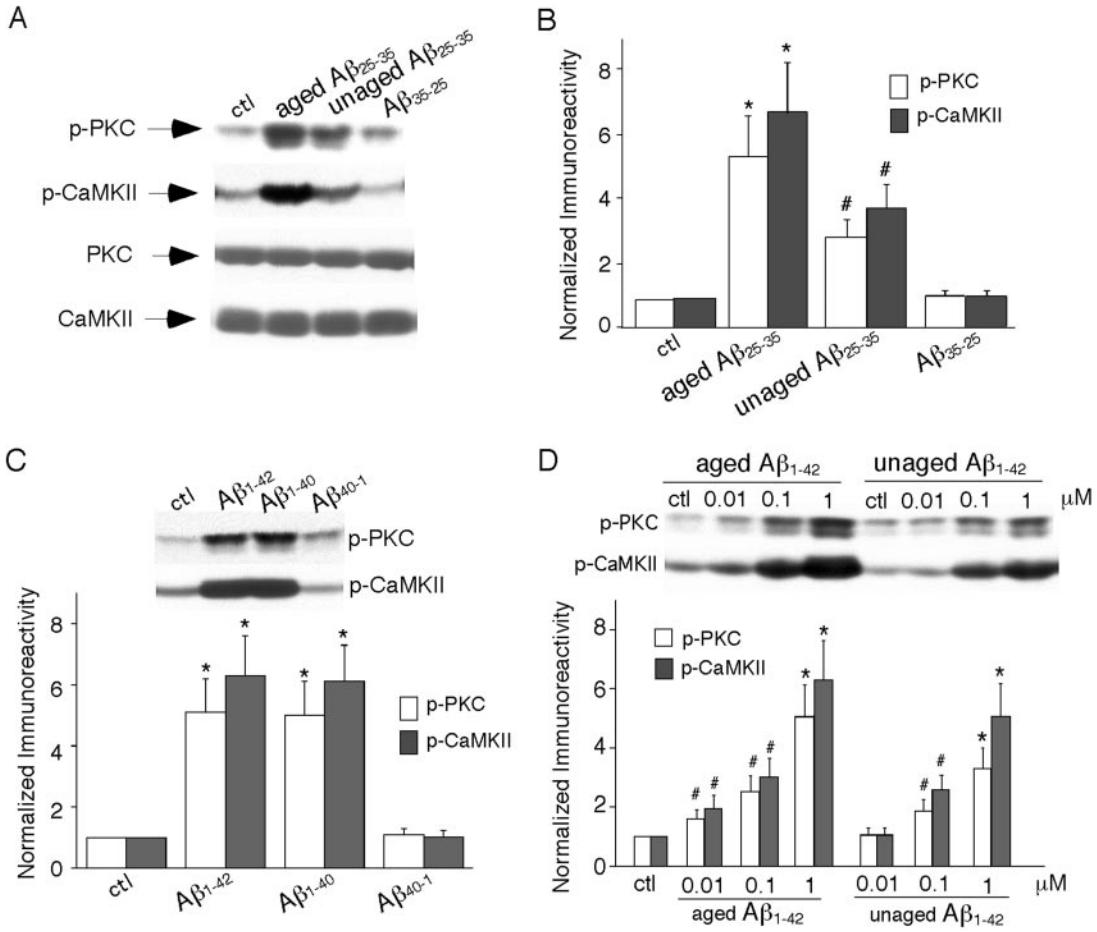

FIG. 2. **Activation of PKC and CaMKII by different Aβ peptides.** *A*, immunoblots of phospho-PKC and phospho-CaMKII. The brain slices were incubated in the absence or presence of aged $A\beta_{25-35}$ (10 μM), unaged $A\beta_{25-35}$ (10 μM), or the aged control peptide $A\beta_{35-25}$ (10 μM) for 10 min. Extracts of the slices were immunoblotted with an anti-phospho-PKC or an anti-phospho-CaMKII antibody, followed by reblotting with antibodies recognizing the total PKC or CaMKII. *B*, quantitation of PKC and CaMKII phosphorylation induced by different Aβ peptides. *C*, quantitation from five experiments showing the activation of PKC and CaMKII by the full-length fibrillar $A\beta_{1-42}$ (1 μM) or $A\beta_{1-40}$ (1 μM) but not by the control peptide $A\beta_{40-1}$ (1 μM). *Inset*, representative immunoblots from one experiment. *D*, quantitation from four experiments showing PKC and CaMKII phosphorylation induced by unaged $A\beta_{1-42}$ and aged $A\beta_{1-42}$ at different concentrations. *Inset*, representative immunoblots from one experiment. *, $p < 0.001$; #, $p < 0.01$, ANOVA, compared with control. *ctl*, control.

$p < 0.001$, ANOVA). To confirm the specificity of the action of $A\beta_{25-35}$, its control peptide containing the reverse sequence $A\beta_{35-25}$ was used to treat cortical slices. As shown in Fig. 2 (*A* and *B*), the aged control peptide $A\beta_{35-25}$ (10 μM) failed to induce the activation of PKC and CaMKII (PKC, 1.1 ± 0.16-fold; CaMKII, 1.05 ± 0.17-fold; $n = 6$, $p > 0.05$, ANOVA).

As shown in Fig. 2*C*, the 10-min treatment with aged full-length $A\beta_{1-42}$ peptide (1 μM) or $A\beta_{1-40}$ peptide (1 μM), but not the control peptide $A\beta_{40-1}$ (1 μM), also induced a significant increase in activated PKC and CaMKII. To further determine the effects of soluble and fibrillar $A\beta_{1-42}$, we compared the potency of unaged and aged $A\beta_{1-42}$ on PKC and CaMKII activation. Soluable $A\beta_{1-42}$ elicited an observable effect at the concentration of 0.1 μM, whereas fibrillar $A\beta_{1-42}$ as low as 0.01 μM produced a detectable effect (Fig. 2*D*). These data suggest that both soluable $A\beta_{1-42}$ (in the form of monomers and oligomers) and highly insoluble $A\beta_{1-42}$ fibrils are able to activate PKC and CaMKII, and the fibrillar form of $A\beta_{1-42}$ is more potent (~10-fold) than the soluable form.

Aβ Induction of PKC and CaMKII Activation Depends on Excitatory Synaptic Transmission and Ca^{2+} Influx—To reveal the potential mechanisms underlying Aβ-induced activation of PKC and CaMKII, we tested the capability of different channel antagonists to block the Aβ signaling. As shown in Fig. 3 (*A* and *B*), the effect of $A\beta_{25-35}$ (10 μM) on PKC and CaMKII activation was largely reduced by the NMDA receptor antagonist MK-801 (10 μM; PKC, 2.0 ± 0.5-fold; CaMKII, 2.3 ± 0.6-fold; $n = 6$). The non-NMDA glutamate receptor antagonist CNQX (10 μM) also significantly attenuated the $A\beta_{25-35}$ effect (PKC, 1.6 ± 0.4-fold; CaMKII, 1.8 ± 0.43-fold; $n = 6$). Blocking L-type voltage-dependent Ca^{2+} channels (VDCCs) with nifedipine (10 μM) partially decreased the $A\beta_{25-35}$ effect (PKC, 3.1 ± 0.7-fold; CaMKII, 3.5 ± 0.8-fold; $n = 6$). Combined application of all three channel antagonists completely eliminated the $A\beta_{25-35}$ effect (PKC, 1.1 ± 0.2-fold; CaMKII, 1.02 ± 0.21-fold; $n = 5$, $p > 0.05$, ANOVA). Shown in Fig. 3 (*C* and *D*) are the effects of $A\beta_{25-35}$ on PKC and CaMKII activation in the presence of TTX or EGTA. Blocking sodium channels and action potentials with TTX (0.5 μM) abolished the $A\beta_{25-35}$ effect (PKC, 1.05 ± 0.21-fold; CaMKII, 1.02 ± 0.25-fold; $n = 6$, $p > 0.05$, ANOVA). Treating cortical slices with the Ca^{2+} chelator EGTA (2 μM) prevented the $A\beta_{25-35}$ activation of PKC and CaMKII (PKC, 1.3 ± 0.28-fold; CaMKII, 1.1 ± 0.23-fold; $n = 6$, $p > 0.05$, ANOVA). Similarly, the effect of $A\beta_{1-42}$ (1 μM) on PKC and CaMKII activation was almost abolished in the presence of CNQX or EGTA. Quantification data and a representative example are shown in Fig. 3*E*. These results suggest that Aβ-induced activation of PKC and CaMKII is dependent on the elevated excitatory activity in glutamatergic synaptic networks and the ensuing calcium entry through

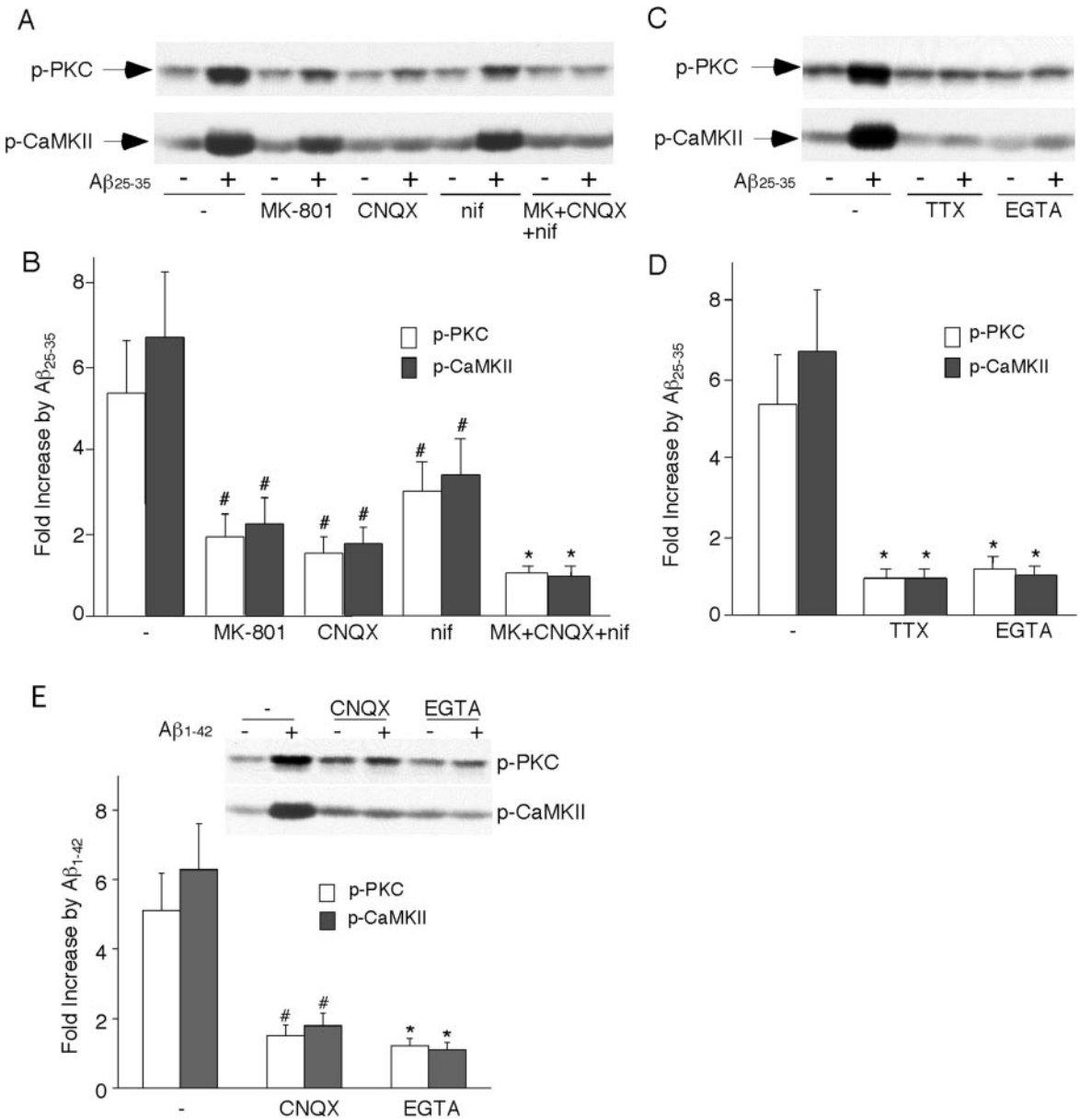

FIG. 3. **Aβ-induced activation of PKC and CaMKII: the role of excitatory transmission.** *A*, immunoblots of phospho-PKC and phospho-CaMKII. The brain slices were preincubated in the absence or presence of various antagonists for 30 min, followed by incubation with or without $A\beta_{25-35}$ (10 μM) for 10 min. PKC and CaMKII phosphorylation induced by $A\beta_{25-35}$ was reduced in the presence of the NMDA receptor antagonist MK-801 (10 μM), the non-NMDA receptor antagonist CNQX (10 μM), or the L-type VDCC antagonist nifedipine (*nif*, 10 μM) and was abolished in the presence of MK-801 + CNQX + nifedipine. *B*, quantitation of $A\beta_{25-35}$-induced fold increase of PKC and CaMKII phosphorylation. *, $p < 0.001$; #, $p < 0.01$, ANOVA, compared with the $A\beta_{25-35}$ effect under control conditions (−). *C*, immunoblots of phospho-PKC and phospho-CaMKII. The brain slices were preincubated in the absence or presence of TTX (0.5 μM) or EGTA (2 μM) for 30 min, followed by incubation with or without $A\beta_{25-35}$ (10 μM) for 10 min. PKC and CaMKII phosphorylation induced by $A\beta_{25-35}$ was eliminated in the presence of the sodium channel blocker TTX or calcium chelator EGTA. *D*, quantitation of $A\beta_{25-35}$-induced fold increase of PKC and CaMKII phosphorylation. *, $p < 0.001$, ANOVA, compared with the $A\beta_{25-35}$ effect under control conditions (−). *E*, quantitation from four experiments showing the blockade of $A\beta_{1-42}$-induced (1 μM) increase of PKC and CaMKII phosphorylation by CNQX and EGTA. *Inset*, representative immunoblots from one experiment. *, $p < 0.001$; #, $p < 0.01$, ANOVA, compared with the $A\beta_{1-42}$ effect under control conditions (−).

glutamate receptor channels and VDCCs.

The Aβ-induced Increase in Activated PKC and CaMKII Is Inhibited by Activation of M1 Muscarinic Receptors—We next examined what can regulate the Aβ signaling in cortical circuits. Because enhancing cholinergic transmission is the most effective therapeutic strategy in AD treatment (26, 27), we first tested the capability of muscarinic (mAChR) and nicotinic (nAChR) receptor agonists to block the Aβ effect. As shown in Fig. 4*A*, pretreatment of cortical slices with the mAChR agonist oxo-M (10 μM, 30 min) almost completely abolished the $A\beta_{25-35}$-induced activation of PKC (0.95 ± 0.23-fold, $n = 8$, $p > 0.05$, ANOVA) and CaMKII (0.9 ± 0.21-fold, $n = 8$, $p > 0.05$, ANOVA). In contrast, the nAChR agonist nicotine (10 μM, 30 min) did not affect the $A\beta_{25-35}$ activation of PKC (5.0 ± 1.3-fold, $n = 5$, $p < 0.001$, ANOVA) and CaMKII (6.2 ± 1.5-fold, $n = 5$, $p < 0.001$, ANOVA). Similarly, the 5-HT_2 serotonin receptor agonist 2,5-dimethoxy-4-iodoamphetamine (DOI) (10 μM, 30 min) also failed to affect the $A\beta_{25-35}$ activation of PKC (5.5 ± 1.4-fold, $n = 6$, $p < 0.001$, ANOVA) and CaMKII (6.8 ± 1.6-fold, $n = 6$, $p < 0.001$, ANOVA).

Among the five subtypes of mAChRs, M1–M5 (38), all types apart from M5 are expressed in cortical neurons (39, 40). We then determined the potential mAChR subtype(s) involved in the regulation of Aβ signaling using specific antagonists. As

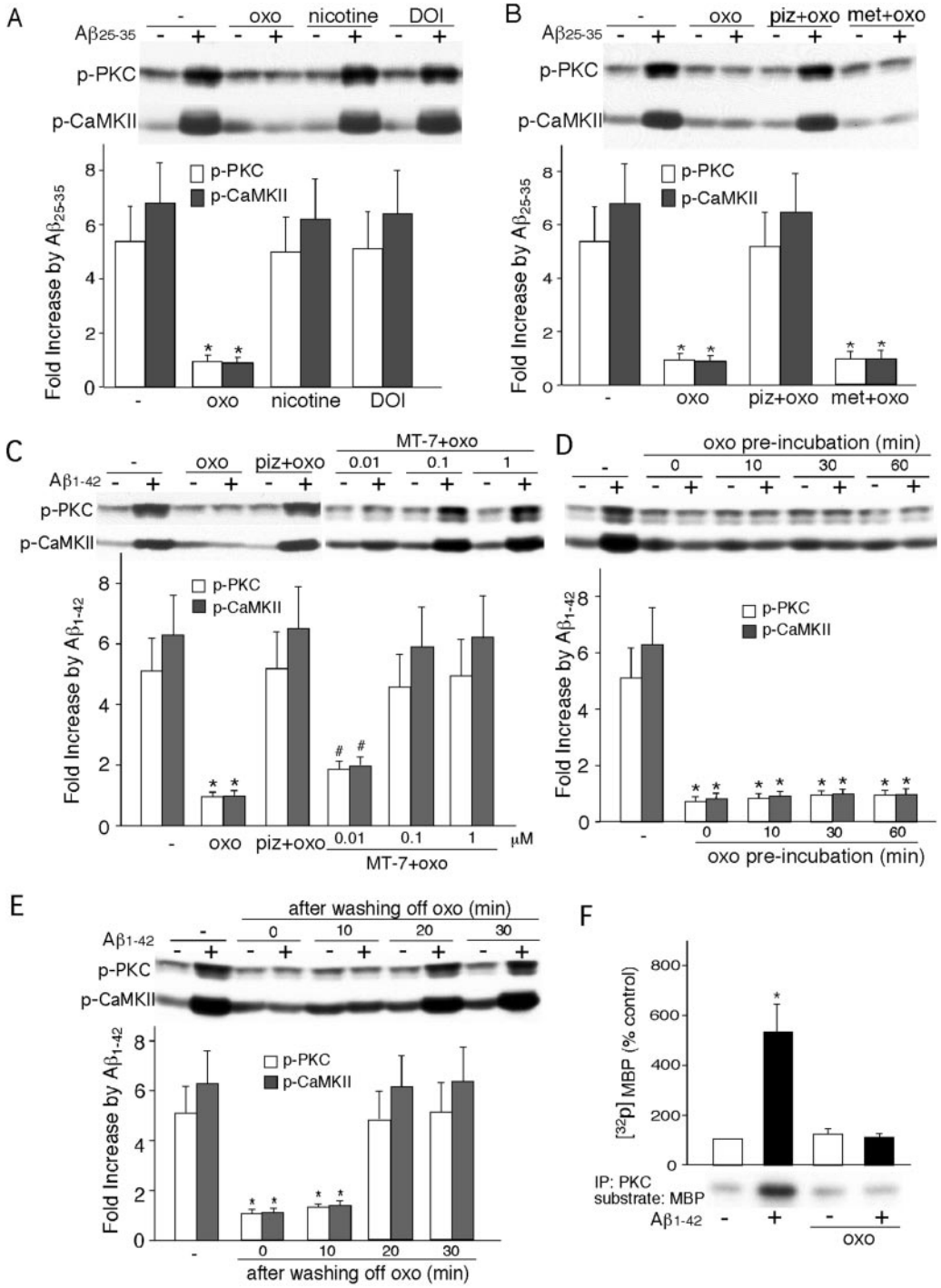

FIG. 4. **Regulation of Aβ-induced PKC and CaMKII activation: the role of M1 mAChRs.** *A* and *B*, quantitation of $A\beta_{25-35}$-induced fold increase of PKC and CaMKII phosphorylation. The brain slices were preincubated in the absence or presence of various agents for 30 min, followed by incubation with or without $A\beta_{25-35}$ (10 μM) for 10 min. PKC and CaMKII phosphorylation induced by $A\beta_{25-35}$ was abolished in the presence of the mAChR agonist oxo-M (*oxo*, 10 μM, *A*) but was unaffected by the nAChR agonist nicotine (10 μM, *A*) or the serotonin (5-HT_2) receptor agonist DOI (10 μM, *A*). The M1/M4 antagonist pirenzepine (*piz*, 10 μM, *B*), but not the M2 antagonist methoctramine (*met*, 10 μM, *B*), eliminated the capability of oxo-M to inhibit $A\beta_{25-35}$-induced phosphorylation of PKC and CaMKII. *Insets* (*A* and *B*), representative immunoblots from single experiments. *, $p < 0.001$, ANOVA, compared with the $A\beta_{25-35}$ effect under control conditions (−). *C*, quantitation showing that oxo-M inhibited the $A\beta_{1-42}$-induced (1 μM) increase of PKC and CaMKII phosphorylation, and this effect of oxo-M was blocked by pirenzepine (10 μM) and the highly selective M1 antagonist MT-7. Different concentrations of MT-7 (0.01, 0.1, and 1 μM) were tested. *D*, quantitation showing the effect of oxo-M preincubation for different durations on $A\beta_{1-42}$-induced (1 μM) increase of PKC and CaMKII phosphorylation. The brain slices were pretreated with oxo-M (10 μM) for different durations (0–60 min), followed by incubation with $A\beta_{1-42}$ (1 μM) for 10 min. All the treatment with oxo-M blocked the $A\beta_{1-42}$ activation of PKC and CaMKII. *E*, quantitation showing the recovery kinetics of the $A\beta_{1-42}$-induced (1 μM) increase of PKC and CaMKII phosphorylation after washing off oxo-M. The brain slices were pretreated with oxo-M (10 μM) for 30 min, and then the oxo-M was washed off. Different lengths of time (0–30 min) elapsed before $A\beta_{1-42}$ (1 μM) was added and incubated for 10 min. About 20 min after washing off oxo-M, $A\beta_{1-42}$ was able to activate PKC and CaMKII. *Insets* (*C–E*), representative immunoblots from single experiments. *, $p < 0.001$; #, $p < 0.01$, ANOVA, compared with the $A\beta_{1-42}$ effect under control conditions (−). *F*, histogram summary of the phosphorylation of PKC substrates in cortical slices treated with or without $A\beta_{1-42}$ in the absence or presence of oxo-M ($n = 4$; *, $p < 0.001$, ANOVA). Cortical slices that have been pretreated with or without oxo-M (10 μM, 30 min) were incubated with or without aged $A\beta_{1-42}$ (1 μM) for 10 min. Lysates of these slices were used for immunoprecipitation with anti-PKC. PKC kinase activity of the immune complex was measured using myelin basic protein (*MBP*) as the substrate. *Inset*, *in vitro* kinase activity of PKC immunoprecipitates from one experiment.

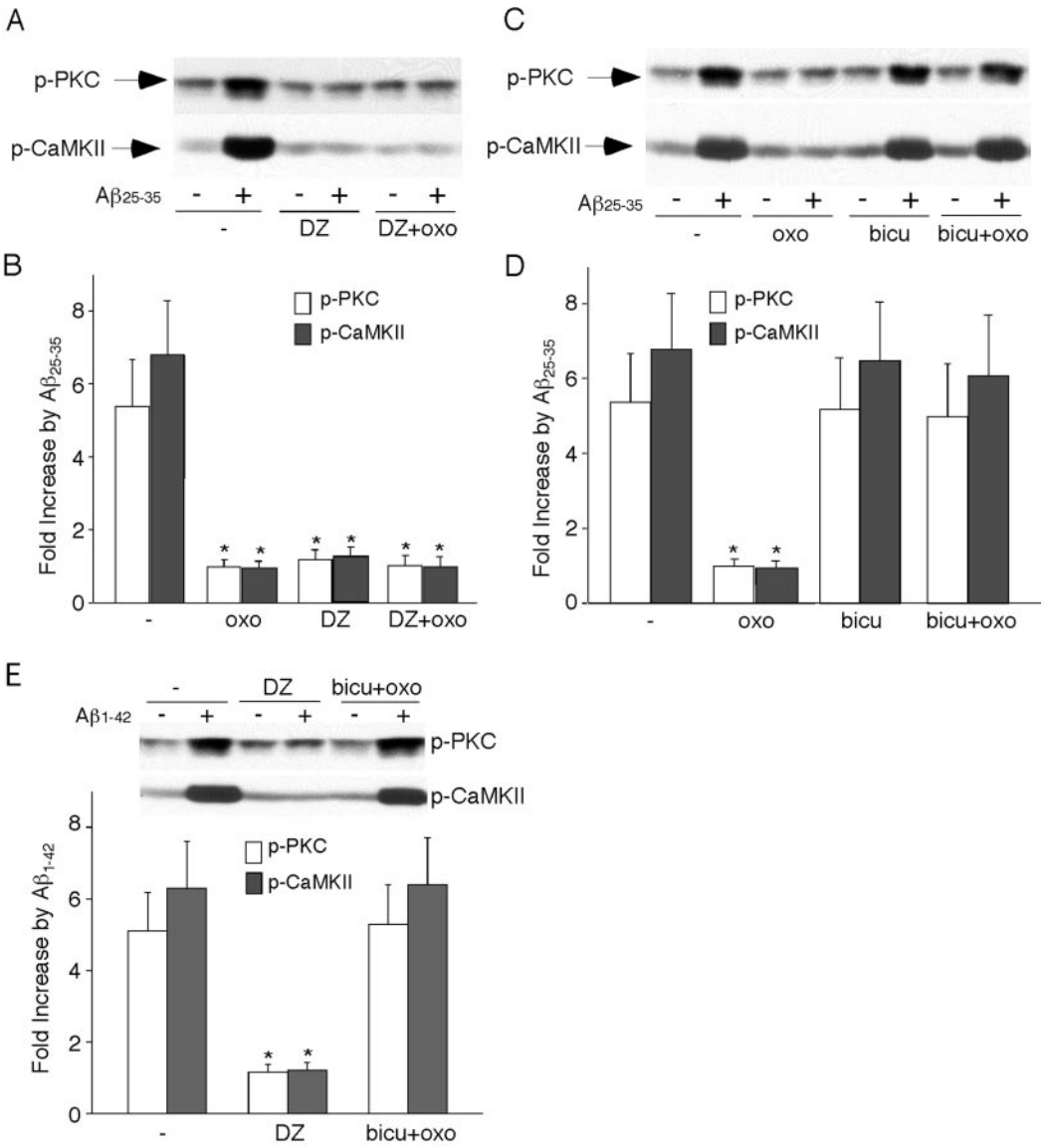

FIG. 5. **Muscarinic regulation of Aβ-induced PKC and CaMKII activation: the role of inhibitory transmission.** *A* and *C*, immunoblots of phospho-PKC and phospho-CaMKII. The brain slices were preincubated in the absence or presence of various agents for 30 min, followed by incubation with or without $A\beta_{25-35}$ (10 μM) for 10 min. The $GABA_A$ receptor enhancer diazepam (*DZ*, 5 μM, *A*) abolished the $A\beta_{25-35}$-induced PKC and CaMKII phosphorylation and occluded the effect of oxo-M (*oxo*, 10 μM, *A*). In the presence of the $GABA_A$ receptor antagonist bicuculline (*bicu*, 5 μM, *C*), oxo-M failed to inhibit $A\beta_{25-35}$-induced phosphorylation of PKC and CaMKII. *B* and *D*, quantitation of $A\beta_{25-35}$-induced fold increase of PKC and CaMKII phosphorylation. *, $p < 0.001$, ANOVA, compared with the $A\beta_{25-35}$ effect under control conditions (−). *E*, quantitation from four experiments showing that diazepam suppressed the $A\beta_{1-42}$-induced (1 μM) increase of PKC and CaMKII phosphorylation, and the inhibitory effect of oxo-M on $A\beta_{1-42}$ activation of PKC and CaMKII was blocked by bicuculline. *Inset*, representative immunoblots from one experiment. *, $p < 0.001$, ANOVA, compared with the $A\beta_{1-42}$ effect under control conditions (−).

shown in Fig. 4*B*, in the presence of the M1/M4 antagonist pirenzepine (1–10 μM), oxo-M lost the ability to inhibit $A\beta_{25-35}$-induced activation of PKC (5.2 ± 1.3-fold, $n = 6$, $p < 0.001$, ANOVA) and CaMKII (6.5 ± 1.45-fold, $n = 6$, $p < 0.001$, ANOVA). On the contrary, the M2 antagonist methoctramine (10 μM) did not prevent the oxo-M inhibition of $A\beta_{25-35}$ activation of PKC (0.99 ± 0.28-fold, $n = 6$, $p > 0.05$, ANOVA) and CaMKII (0.97 ± 0.31-fold, $n = 6$, $p > 0.05$, ANOVA). Similarly, the $A\beta_{1-42}$-induced activation of PKC and CaMKII was also significantly inhibited by oxo-M, and this effect of oxo-M was blocked by pirenzepine (Fig. 4*C*). Given the limited selectivity of pirenzepine (~5-fold) for M1 and M4 receptors (41, 42), we used MT-7, a highly selective (>10,000-fold) ligand for M1 receptors (43), to confirm the involvement of M1 receptors. As shown in Fig. 4*C*, MT-7 (0.1 μM) eliminated the ability of oxo-M to inhibit $A\beta_{1-42}$ activation of PKC (4.3 ± 1.6-fold, $n = 4$, $p < 0.001$, ANOVA) and CaMKII (5.9 ± 1.7-fold, $n = 4$, $p < 0.001$, ANOVA), indicating that the effect of oxo-M is mediated by M1 receptors. These results thus suggest that activation of M1 receptors can block Aβ signaling in cortical networks.

To further analyze the inhibition of Aβ actions by muscarinic stimulation, we pretreated cortical slices with oxo-M for different durations (0, 10, 30, and 60 min) before adding $A\beta_{1-42}$ and incubated for 10 min. As shown in Fig. 4*D*, no matter how long the pretreatment with oxo-M was (0–60 min), subsequent addition of $A\beta_{1-42}$ failed to induce any further activation of PKC and CaMKII. There was a small activation of PKC and CaMKII during the initial muscarinic stimulation, but the muscarinic action returned to base line after 10–30 min. These data suggest that the constant presence of muscarinic activation prevents the Aβ-initiated signaling. When we pretreated cortical slices with oxo-M and then washed it out to prevent further muscarinic activation, subsequent addition of $A\beta_{1-42}$ regained the ability to activate PKC and CaMKII after 20 min (Fig. 4*E*).

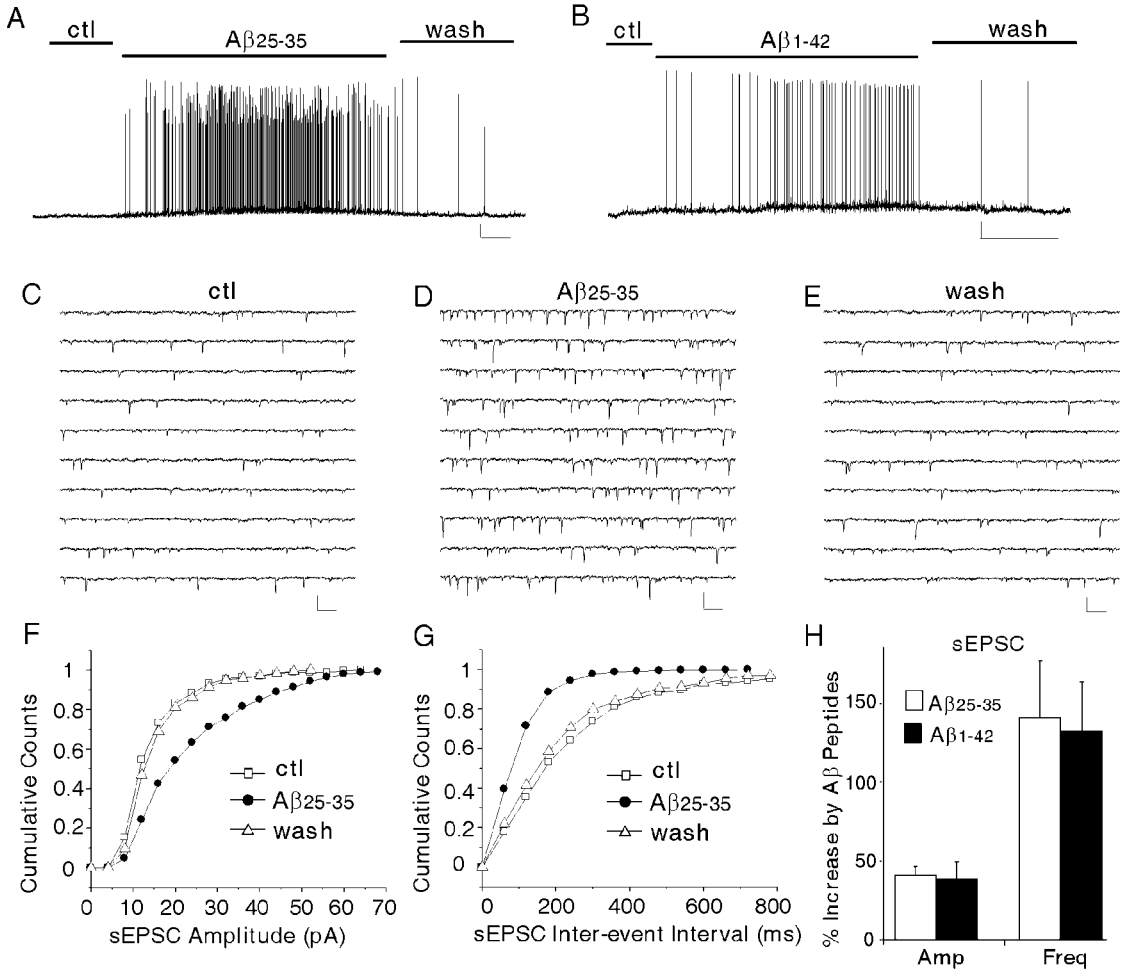

FIG. 6. **$A\beta_{25-35}$-induced changes in membrane excitability and excitatory synaptic transmission in frontal cortical pyramidal neurons.** *A* and *B*, whole cell current clamp recordings showing that exposure to aged $A\beta_{25-35}$ (10 μM, *A*) or $A\beta_{1-42}$ (2 μM, *B*) induced a slight depolarization and triggered bursts of action potentials. *Scale bars*, 10 mV, 1 min. *C–E*, representative sEPSC traces recorded from a voltage-clamped cortical pyramidal neuron under control condition (*C*), during bath application of $A\beta_{25-35}$ (*D*), and after washing off the peptide (*E*). *Scale bars*, 50 pA, 100 ms. *F* and *G*, cumulative plots indicating that the distribution of sEPSC amplitude (*F*) and frequency (*G*) was reversibly increased by $A\beta_{25-35}$ in the neuron. *H*, histograms (means ± S.E.) showing the percentages of increase of sEPSC amplitude (*Amp*) and frequency (*Freq*) by $A\beta_{25-35}$ ($n = 8$) and $A\beta_{1-42}$ ($n = 5$). *ctl*, control.

We also performed *in vitro* kinase assay to confirm that the $A\beta_{1-42}$ activation of PKC can be blocked by muscarinic stimulation. As shown in Fig. 4*F*, application of aged $A\beta_{1-42}$ (1 μM, 10 min) to cortical slices induced a potent increase of PKC catalytic activity, as measured by the phosphorylation of its substrate myelin basic protein (5.2 ± 0.9-fold, $n = 4$, $p < 0.001$, ANOVA), consistent with the results obtained with the PKC phosphospecific antibody. Pretreatment of cortical slices with oxo-M (10 μM, 30 min) abolished the $A\beta_{1-42}$-induced activation of PKC with the enzymatic assay (0.98 ± 0.1-fold, $n = 4$, $p > 0.05$, ANOVA).

Muscarinic Receptors Block Aβ Signaling through the Enhancement of GABAergic Inhibitory Transmission—What might account for the muscarinic inhibition of Aβ signaling? Because the Aβ activation of PKC and CaMKII appears to be dependent on the enhanced glutamatergic excitatory synaptic activity (Fig. 3), muscarinic receptors should attenuate the Aβ effect if they can enhance the counteracting GABAergic inhibitory synaptic activity. We therefore tested the oxo-M effect on Aβ signaling when the GABA system is manipulated. As shown in Fig. 5 (*A* and *B*), application of the $GABA_A$ receptor enhancer diazepam (5 μM) exerted a similar effect as oxo-M: blocking the $A\beta_{25-35}$-induced activation of PKC (1.2 ± 0.27-fold, $n = 6$, $p > 0.05$, ANOVA) and CaMKII (1.25 ± 0.29-fold, $n = 6$, $p > 0.05$, ANOVA). Moreover, diazepam largely occluded the effect of subsequent oxo-M application (PKC, 1.02 ± 0.26-fold; CaMKII, 0.98 ± 0.28-fold; $n = 5$, $p > 0.05$, ANOVA). To further confirm that the oxo-M suppression of $A\beta_{25-35}$ signaling is dependent on the muscarinic enhancement of GABAergic inhibition, we blocked $GABA_A$ receptor channels with bicuculline (5 μM). As shown in Fig. 5 (*C* and *D*), in the presence of bicuculline, oxo-M failed to inhibit $A\beta_{25-35}$-induced activation of PKC (5.1 ± 1.4-fold, $n = 6$, $p < 0.001$, ANOVA) and CaMKII (6.1 ± 1.6-fold, $n = 6$, $p < 0.001$, ANOVA). Likewise, diazepam also blocked the $A\beta_{1-42}$-induced activation of PKC and CaMKII (Fig. 5*E*), mimicking the inhibitory effect of oxo-M on $A\beta_{1-42}$ signaling (Fig. 4*E*). Moreover, bicuculline prevented the oxo-M inhibition of $A\beta_{1-42}$ activation of PKC and CaMKII (Fig. 5*E*). These data suggest the requirement of GABAergic inhibitory synaptic transmission in the muscarinic regulation of Aβ actions.

To provide more direct evidence for the mechanisms underlying muscarinic inhibition of Aβ signaling, we performed electrophysiological experiments to test the impact of Aβ and oxo-M on excitatory and inhibitory transmission in cortical slices. The synaptic activity of frontal cortical pyramidal neurons in response to Aβ exposure was first examined using whole cell current clamp recordings. As shown in Fig. 6 (*A* and *B*), bath application of $A\beta_{25-35}$ (10 μM) or $A\beta_{1-42}$ (2 μM) induced excitatory postsynaptic potentials and triggered sustained action potentials ($A\beta_{25-35}$, $n = 8$; $A\beta_{1-42}$, $n = 5$). Furthermore,

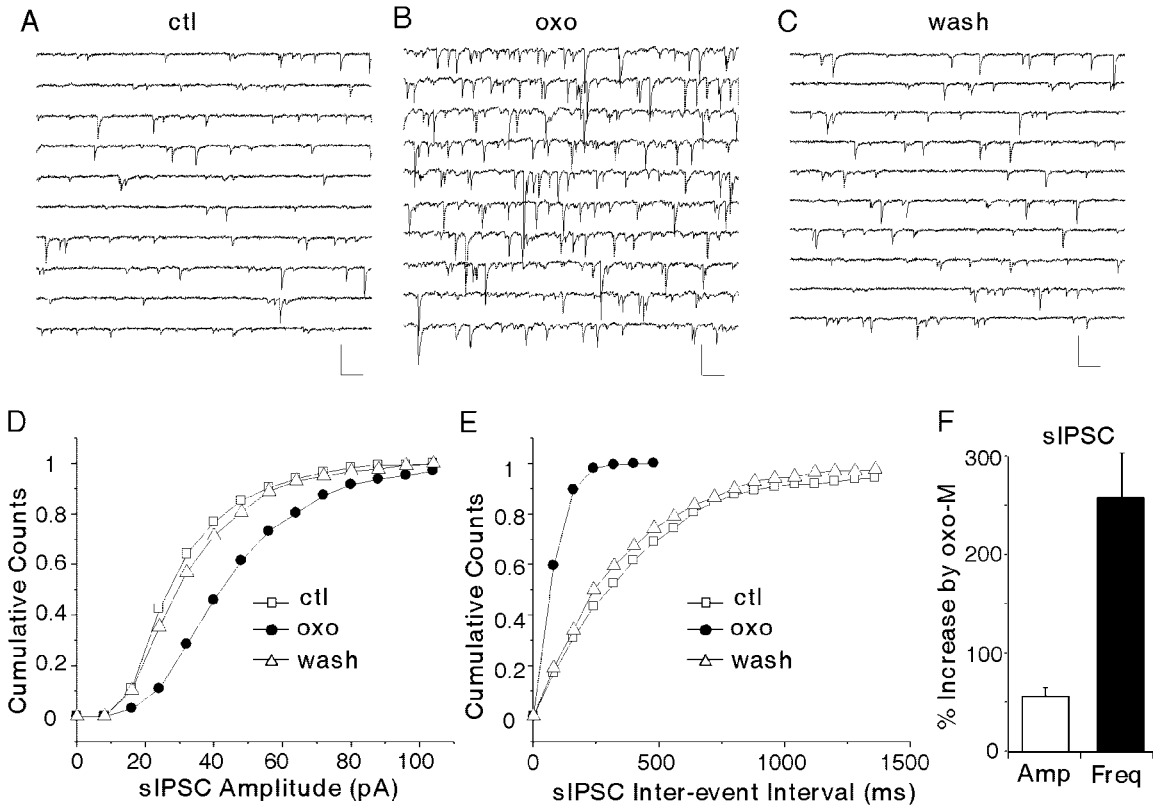

FIG. 7. **Effects of muscarinic receptors on inhibitory synaptic transmission in frontal cortical pyramidal neurons.** *A–C*, representative sIPSC traces recorded from a voltage-clamped cortical pyramidal neuron under control conditions (*A*), during bath application of oxo-M (20 μM) (*B*), and after washing off the agonist (*C*). *Scale bars*, 100 pA, 100 ms. *D* and *E*, cumulative plots indicating that the distribution of sIPSC amplitude (*D*) and frequency (*E*) was reversibly increased by oxo-M in the neuron. *F*, histograms (means ± S.E.) showing the percentages of increase of sIPSC amplitude (*Amp*) and frequency (*Freq*) by oxo-M ($n = 7$). *ctl*, control.

whole cell voltage clamp recordings show that $A\beta_{25-35}$ (10 μM) or $A\beta_{1-42}$ (2 μM) caused a marked increase in the frequency and amplitude of sEPSCs. A representative example is shown in Fig. 6 (*C–G*). As summarized in Fig. 6*H*, in a sample of neurons examined, $A\beta_{25-35}$ increased the mean sEPSC amplitude by 42.9 ± 5.5% (mean ± S.E., $n = 8$, $p < 0.001$, K-S test) and the mean sEPSC frequency by 141.9 ± 39.1% ($n = 8$, $p < 0.001$, K-S test). Similarly, $A\beta_{1-42}$ increased the mean sEPSC amplitude by 40.5 ± 10.2% ($n = 5$, $p < 0.001$, K-S test) and the mean sEPSC frequency by 131.9 ± 30.1% ($n = 5$, $p < 0.001$, K-S test). In contrast to the potent enhancement of sEPSCs, $A\beta_{25-35}$ had no effect on sIPSCs ($n = 6$, data not shown). On the other hand, oxo-M induced a potent increase in the frequency and amplitude of sIPSCs. A representative example is shown in Fig. 7 (*A–E*). As summarized in Fig. 7*F*, in a sample of neurons examined, oxo-M increased the mean amplitude of sIPSCs by 52.3 ± 9.3% (mean ± S.E., $n = 7$, $p < 0.001$, K-S test) and the mean frequency of sIPSCs by 256.1 ± 48.4% ($n = 7$, $p < 0.001$, K-S test). Taken together, these results suggest that Aβ exposure activates excitatory synapses in cortical circuits, and muscarinic receptors enhance the counteracting inhibitory transmission, which could lead to the blockade of the Aβ signaling.

DISCUSSION

Aβ-induced Signaling in Cortical Neurons—Since the discovery of the link between Aβ deposits and AD, therapeutic strategies have been aiming at reducing the brain amyloid burden (14, 15). Aβ is synthesized and secreted by brain cells (44, 45). The neurotoxicity after prolonged exposure to high concentrations of Aβ has been established in *in vitro* models (10, 11). However, accumulation of diffuse deposits of Aβ in the brain is an early event in the development of AD when there is no massive neuronal death, emphasizing the importance of elucidating the initial neuronal responses to Aβ fibrils that precede neurodegeneration. The significance of understanding the physiological roles of Aβ apart from its neurotoxic effects is perhaps more clear in aged APP transgenic mice (46), where numerous Aβ plaques are seen in cortical and limbic structures; yet deficits in synaptic plasticity and spatial working memory are accompanied by minimal or no loss of presynaptic or postsynaptic elements (47, 48). Therefore, the Aβ-induced dysfunction of cortical and hippocampal neurons, not their death, may be largely responsible for the impairments in learning and memory associated with AD.

Previous studies have found that Aβ administration induced a marked increase in the tyrosine phosphorylation of multiple proteins in nerve cell lines and cortical cultures (49–51), suggesting that Aβ has the potential to modulate cellular responses to growth factors and extracellular matrix molecules. In this study, we report a rapid and potent activation of two important serine/threonine kinases, PKC and CaMKII, in response to $A\beta_{25-35}$, $A\beta_{1-42}$, and $A\beta_{1-40}$ in cortical slices. The fibrillar Aβ peptides ($A\beta_{25-35}$ and $A\beta_{1-42}$) were shown to be more potent than their soluable forms in eliciting the activation of PKC and CaMKII, whereas the full-length $A\beta_{1-42}$ and $A\beta_{1-40}$ were found to be more potent than $A\beta_{25-35}$ in this process. The $A\beta_{25-35}$ activation of PKC and CaMKII was not found in HEK293 cell lines (data not shown), indicative of the requirement of some neural specific elements in the Aβ action. Because PKC and CaMKII activation could change the phosphorylation state and functional properties of many downstream targets including neurotransmitter receptors, ion channels, presynaptic terminal proteins, and cytoskeletal molecules

(52–54), Aβ might modulate a wide variety of neuronal functions ranging from synaptic plasticity and transmitter release to neurite outgrowth via the regulation of PKC and CaMKII.

Mechanisms for Aβ Signaling—One of the major mechanisms for the Aβ-induced cell death is calcium overload and disruption of calcium homeostasis (55). In this study, pharmacological evidence suggests that Aβ activation of PKC and CaMKII is dependent on Ca^{2+} influx resulting from Aβ-induced excitation of glutamatergic synapses, consistent with previous calcium imaging results showing that application of $A\beta_{25-35}$ to cultured hippocampal neurons caused increases in the intracellular Ca^{2+} (56). Several agents that interfere with glutamatergic transmission, including CNQX, MK-801, and TTX, were effective in eliminating or reducing the Aβ activation of PKC and CaMKII, whereas blocking GABAergic transmission with bicuculline was without effect (Fig. 5, *C* and *D*), indicating that the Aβ action specifically required activation of the excitatory network. Following Aβ activation of glutamate synapses, Ca^{2+} could enter via several routes, including NMDA receptors, VDCCs, and Ca^{2+}-permeable AMPA/KA receptors.

Parallel electrophysiological studies in cortical pyramidal neurons show that application of Aβ induced excitatory postsynaptic potentials and bursts of action potentials, indicating that Aβ elevated the excitability of these glutamatergic projection neurons. Neither AMPA- nor NMDA-evoked currents were significantly affected by $A\beta_{25-35}$ (data not shown), suggesting a lack of effect of Aβ on postsynaptic glutamate receptor activity. The Aβ-induced increase in sEPSC frequency and amplitude confirms that Aβ caused an increase in glutamate release in cortical circuits. Previous studies have shown that Aβ induces Ca^{2+} influx through VDCCs in cortical neurons and nerve cell lines (57, 58), activates large, nonselective cation currents in sympathetic and cortical neurons (59, 60), and inhibits several potassium currents in basal forebrain cholinergic neurons (61). Thus the Aβ-induced alteration of cellular ionic activity through interaction with existing channels or *de novo* channel formation (62) might be one of the key mechanisms underlying the Aβ activation of neuronal excitability.

Regulation of Aβ Signaling by Muscarinic Receptors—Given the strong activation of PKC and CaMKII by fibrillar Aβ, it is important to know what can potentially modulate this signaling. Our data suggest that activation of muscarinic receptors potently down-regulated the Aβ action, and this effect was specific for M1 receptors. Furthermore, Aβ lost the ability to activate PKC and CaMKII as long as there was constant M1 receptor activation. About 20 min after M1 receptors were inactivated, the ability of Aβ to activate PKC and CaMKII recovered. Therefore, activation of muscarinic receptors will not only modify APP processing and inhibit Aβ production (22, 23, 63) but also suppress Aβ functioning (the present study). The cholinergic deficiency in AD brains could lead to the loss of this negative regulation of amyloidogenic Aβ, which in turn could impair M1 signal transduction (64, 65) and inhibit ACh synthesis and release (66, 67), aggravating further the cholinergic hypofunction (21). Because these "vicious cycles" could potentially be inhibited by M1 agonists, it suggests that enhancing M1 signaling is a promising point of pharmacological intervention in the treatment of AD (68, 69).

Mechanisms for Muscarinic Regulation of Aβ Signaling—Previous studies have shown that activation of muscarinic receptors increases the excitability of cortical GABAergic interneurons (70, 71). Because the Aβ activation of PKC and CaMKII was dependent on enhanced excitatory glutamatergic transmission, we postulated that enhancing the GABAergic inhibitory synaptic activity may account for the muscarinic inhibition of Aβ signaling. Both pharmacological and electrophysiological evidence supports this hypothesis. Several manipulations that interfere with GABA transmission, such as enhancing postsynaptic responses to GABA with diazepam or blocking $GABA_A$ receptor functions with bicuculline, were effective in mimicking or blocking the muscarinic inhibition of Aβ signaling, respectively. Moreover, muscarinic agonists potently increased inhibitory postsynaptic currents recorded in pyramidal neurons of frontal cortex. By potentiating GABA inhibition to counteract the elevated glutamate excitation elicited by Aβ exposure, muscarinic receptors not only abrogated the Aβ activation of PKC and CaMKII but also can potentially suppress the Aβ-induced susceptibility to excitatoxicity in cortical circuits.

Acknowledgment—We thank Xiaoqing Chen for technical support.

REFERENCES

1. Masters, C. L., Simms, G., Weinman, N. A., Multhaup, G., McDonald, B. L., and Beyreuther, K. (1985) *Proc. Natl. Acad. Sci. U. S. A.* **82,** 4245–4249
2. Small, D. H., Mok, S. S., and Bornstein, J. C. (2001) *Nat. Rev. Neurosci.* **2,** 595–598
3. Sommer, B. (2002) *Curr. Opin. Pharmacol.* **2,** 87–92
4. Selkoe, D. J. (1998) *Trends Cell Biol.* **8,** 447–453
5. Selkoe, D. J. (1996) *J. Biol. Chem.* **271,** 18295–18298
6. Tanzi, R. E., and Bertram, L. (2001) *Neuron* **32,** 181–184
7. Games, D., Adams, D., Alessandrini, R., Barbour, R., Berthelette, P., Blackwell, C., Carr, T., Clemens, J., Donaldson, T., and Gillespie, F. (1995) *Nature* **373,** 523–527
8. Hsiao, K., Chapman, P., Nilsen, S., Eckman, C., Harigaya, Y., Younkin, S., Yang, F., and Cole, G. (1996) *Science* **274,** 99–103
9. Chen, G., Chen, K. S., Knox, J., Inglis, J., Bernard, A., Martin, S. J., Justice, A., McConlogue, L., Games, D., Freedman, S. B., and Morris, R. G. (2000) *Nature* **408,** 975–979
10. Yankner, B. A., Dawes, L. R., Fisher, S., Villa-Komaroff, L., Oster-Granite, M. L., and Neve, R. L. (1989) *Science* **245,** 417–420
11. Pike, C. J., Walencewicz, A. J., Glabe, C. G., and Cotman, C. W. (1991) *Brain Res.* **563,** 311–314
12. Koh, J. Y., Yang, L. L., and Cotman, C. W. (1990) *Brain Res.* **533,** 315–320
13. Mattson, M. P., Cheng, B., Davis, D., Bryant, K., Lieberburg, I., and Rydel, R. E. (1992) *J. Neurosci.* **12,** 376–389
14. Vassar, R., and Citron, M. (2000) *Neuron* **27,** 419–422
15. Esler, W. P., and Wolfe, M. S. (2001) *Science* **293,** 1449–1454
16. Whitehouse, P. J., Price, D. L., Clark, A. W., Coyle, J. T., and DeLong, M. R. (1981) *Ann. Neurol.* **10,** 122–126
17. Whitehouse, P. J., Price, D. L., Struble, R. G., Clark, A. W., Coyle, J. T., and Delon, M. R. (1982) *Science* **215,** 1237–1239
18. Coyle, J. T., Price, D. L., and DeLong, M. R. (1983) *Science* **219,** 1184–1190
19. Nathanson, N. M. (1987) *Annu. Rev. Neurosci.* **10,** 195–236
20. Winkler, J., Suhr, S. T., Gage, F. H., Thal, L. J., and Fisher, L. J. (1995) *Nature* **375,** 484–487
21. Auld, D. S., Kar, S., and Quirion, R. (1998) *Trends Neurosci.* **21,** 43–49
22. Hung, A. Y., Haass, C., Nitsch, R. M., Qiu, W. Q., Citron, M., Wurtman, R. J., Growdon, J. H., and Selkoe, D. J. (1993) *J. Biol. Chem.* **268,** 22959–22962
23. Lin, L., Georgievska, B., Mattsson, A., and Isacson, O. (1999) *Proc. Natl. Acad. Sci. U. S. A.* **96,** 12108–12113
24. Tanaka, C., and Nishizuka, Y. (1994) *Annu. Rev. Neurosci.* **17,** 551–567
25. Soderling, T. R. (2000) *Curr. Opin. Neurobiol.* **10,** 375–380
26. Sitaram, N., Weingartner, H., and Gillin, J. C. (1978) *Science* **201,** 274–276
27. Weinstock, M. (1995) *Neurodegeneration* **4,** 349–356
28. Feng, J., Cai, X., Zhao, J., and Yan, Z. (2001) *J. Neurosci.* **21,** 6502–6511
29. Cai, X., Flores-Hernandez, J., Feng, J., and Yan, Z. (2002) *J. Physiol.* (*Lond.*) **540,** 743–759
30. Terzi, E., Holzemann, G., and Seelig, J. (1994) *Biochemistry* **33,** 1345–1350
31. Serpell, L. C. (2000) *Biochim. Biophys. Acta* **1502,** 16–30
32. Combs, C. K., Johnson, D. E., Cannady, S. B., Lehman, T. M., and Landreth, G. E. (1999) *J. Neurosci.* **19,** 928–939
33. McDonald, D., Bamberger, M., Combs, C., and Landreth, G. (1998) *J. Neurosci.* **18,** 4451–4460
34. Yankner, B. A., Duffy, L. K., and Kirschner, D. A. (1990) *Science* **250,** 279–282
35. Behn-Krappa, A., and Newton, A. C. (1999) *Curr. Biol.* **9,** 728–737
36. Miller, S. G., and Kennedy, M. B. (1986) *Cell* **44,** 861–870
37. Miller, S. G., Patton, B. L., and Kennedy, M. B. (1988) *Neuron* **1,** 593–604
38. Bonner, T. I., Buckley, N. J., Young, A. C., and Brann, M. R. (1987) *Science* **237,** 527–532
39. Levey, A. I., Kitt, C. A., Simonds, W. F., Price, D. L., and Brann, M. R. (1991) *J. Neurosci.* **11,** 3218–3226
40. Stewart, A. E., Yan, Z., Surmeier, D. J., and Foehring, R. C. (1999) *J. Neurophysiol.* **81,** 72–84
41. Hammer, R., Berrie, C. P., Birdsall, N. J., Burgen, A. S., and Hulme, E. C. (1980) *Nature* **283,** 90–92
42. Buckley, N. J., Bonner, T. I., Buckley, C. M., Brann, M. R. (1989) *Mol. Pharmacol.* **35,** 469–476
43. Adem, A., Karlsson, E. (1997) *Life Sci.* **60,** 1069–1076
44. Haass, C., Schlossmacher, M. G., Hung, A. Y., Vigo-Pelfrey, C., Mellon, A., Ostaszewski, B. L., Lieberburg, I., Koo, E. H., Schenk, D., Teplow, D. B., *et al.* (1992) *Nature* **359,** 322–325
45. Seubert, P., Vigo-Pelfrey, C., Esch, F., Lee, M., Dovey, H., Davis, D., Sinha, S., Schlossmacher, M., Whaley, J., Swindlehurst, C., *et al.* (1992) *Nature* **359,**

325–327
46. Hsiao, K. (1998) *Prog. Brain Res.* **117,** 335–341
47. Irizarry, M. C., Soriano, F., McNamara, M., Page, K. J., Schenk, D., Games, D., and Hyman, B. T. (1997) *J. Neurosci.* **17,** 7053–7059
48. Chapman, P. F., White, G. L., Jones, M. W., Cooper-Blacketer, D., Marshall, V. J., Irizarry, M., Younkin, L., Good, M. A., Bliss, T. V., Hyman, B. T., Younkin, S. G., and Hsiao, K. K. (1999) *Nat. Neurosci.* **2,** 271–276
49. Luo, Y. Q., Hirashima, N., Li, Y. H., Alkon, D. L., Sunderland, T., Etcheberrigaray, R., and Wolozin, B. (1995) *Brain Res.* **681,** 65–74
50. Zhang, C., Lambert, M. P., Bunch, C., Barber, K., Wade, W. S., Krafft, G. A., and Klein, W. L. (1994) *J. Biol. Chem.* **269,** 25247–25250
51. Williamson, R., Scales, T., Clark, B. R., Gibb, G., Reynolds, C. H., Kellie, S., Bird, I. N., Varndell, I. M., Sheppard, P. W., Everall, I., and Anderton, B. H. (2002) *J. Neurosci.* **22,** 10–20
52. Barria, A., Muller, D., Derkach, V., Griffith, L. C., and Soderling, T. R. (1997) *Science* **276,** 2042–2045
53. Nayak, A. S., Moore, C. I., and Browning, M. D. (1996) *Proc. Natl. Acad. Sci. U. S. A.* **93,** 15451–15456
54. Quinlan, E. M., and Halpain, S. (1996) *J. Neurosci.* **16,** 7627–7637
55. Mattson, M. P., Barger, S. W., Cheng, B., Lieberburg, I., Smith-Swintosky, V. L., and Rydel, R. E. (1993) *Trends Neurosci.* **16,** 409–414
56. Brorson, J. R., Bindokas, V. P., Iwama, T., Marcuccilli, C. J., Chisholm, J. C., and Miller, R. J. (1995) *J. Neurobiol.* **26,** 325–338
57. Davidson, R. M., Shajenko, L., and Donta, T. S. (1994) *Brain Res.* **643,** 324–327
58. Weiss, J. H., Pike, C. J., and Cotman, C. W. (1994) *J. Neurochem.* **62,** 372–375
59. Furukawa, K., Abe, Y., and Akaike, N. (1994) *Neuroreport* **5,** 2016–2018
60. Simmons, M. A., and Schneider, C. R. (1993) *Neurosci. Lett.* **150,** 133–136
61. Jhamandas, J. H., Cho, C., Jassar, B., Harris, K., MacTavish, D., and Easaw, J. (2001) *J. Neurophysiol.* **86,** 1312–1320
62. Fraser, S. P., Suh, Y. H., and Djamgoz, M. B. (1997) *Trends Neurosci.* **20,** 67–72
63. Nitsch, R. M., Slack, B. E., Wurtman, R. J., and Growdon, J. H. (1992) *Science* **258,** 304–307
64. Kelly, J. F., Furukawa, K., Barger, S. W., Rengen, M. R., Mark, R. J., Blanc, E. M., Roth, G. S., and Mattson, M. P. (1996) *Proc. Natl. Acad. Sci. U. S. A.* **93,** 6753–6758
65. Jope, R. S., Song, L., and Powers, R. E. (1997) *Neurobiol. Aging* **18,** 111–120
66. Hoshi, M., Takashima, A., Murayama, M., Yasutake, K., Yoshida, N., Ishiguro, K., Hoshino, T., and Imahori, K. (1997) *J. Biol. Chem.* **272,** 2038–2041
67. Kar, S., Seto, D., Gaudreau, P., and Quirion, R. (1996) *J. Neurosci.* **16,** 1034–1040
68. Fisher, A., Michaelson, D. M., Brandeis, R., Haring, R., Chapman, S., and Pittel, Z. (2000) *Ann. N. Y. Acad. Sci.* **920,** 315–320
69. Messer, W. S., Jr. (2002) *Curr. Top. Med. Chem.* **2,** 353–358
70. Kawaguchi, Y. (1997) *J. Neurophysiol.* **78,** 1743–1747
71. Kondo, S., and Kawaguchi, Y. (2001) *Neurosience* **107,** 551–560